Journal of Applied Polymer Science

On Rheology–Morphology Correlation of Polypropylene/Poly(trimethylene terephthalate) Blend Nanocomposites

H. A. Khonakdar,[1] P. Saen,[1] A. Nodehi,[1] S. H. Jafari,[2] A. Asadinezhad,[3] U. Wagenkncht,[4] G. Heinrich[4,5]

[1]Department of Polymer Processing, Iran Polymer and Petrochemical Institute, 14965-115 Tehran, Iran
[2]School of Chemical Engineering, College of Engineering, University of Tehran, 11365-4563 Tehran, Iran
[3]Department of Chemical Engineering, Isfahan University of Technology, 84156-83111 Isfahan, Iran
[4]Institute of Polymer Materials, Leibniz-Institute of Polymer Research, Dresden D-01067, Germany
[5]Technische Universität Dresden, Institut für Werkstoffwissenschaft, D-01069 Dresden, Germany

Correspondence to: H. A. Khonakdar (E-mail: hakhonakdar@gmail.com)

ABSTRACT: A correlation between rheology and morphology of polypropylene/poly(trimethylene terephthalate) blend nanocomposites was addressed. Organoclay particles were preferentially localized either at the interface or inside the polyester phase depending upon affinity the level and exerted compatibilizing role by making a finer morphology. The functional compatibilizer was found to be highly efficient in giving rise to an enhanced interfacial adhesion and uniform morphology. The compatibilizer also expanded the clay gallery space by increasing its interlayer distance. Rheological measurements showed that nanoclay and compatibilizer contribute to the complex viscosity of the system considerably. Also, an upturn was detected at low angular frequencies ascribed to a secondary structure formation. Similar behavior was also found when storage shear modulus was studied, where at low frequencies a terminal plateau of yield stress character appeared that was connected with some intermolecular networks. This was further supported via relaxation time spectra wherein additional peaks due to interface emerged at low frequencies. © 2012 Wiley Periodicals, Inc. J. Appl. Polym. Sci. 000: 000–000, 2012

KEYWORDS: rheology; morphology; blends; nanocomposites; poly(trimethylene terephthalate)

Received 24 February 2012; accepted 23 March 2012; published online
DOI: 10.1002/app.37776

INTRODUCTION

Blending has yet survived to be an effective, inexpensive approach to deliver novel polymer materials of tailor-made performance for specific applications. When combined with a proper compounding route, blending may exploit the desired properties of each constituent.[1] On the other hand, most homopolymers are intrinsically incompatible from thermodynamic point of view, which results in poor mechanical performance.[2] There have been suggested a variety of techniques to tackle this problem, among which the addition of a compatibilizer is of utmost interest which tune interfacial characteristics with an eye to raise compatibility. This in fact, reduces the interfacial tension between an immiscible pair of polymers leading to finer morphology and enhanced adhesion.[3] The compatibilizers are principally graft and block copolymers dwelled at the interphase region. Nonetheless, the interacting layered nanoparticles, besides improving the physical and mechanical performance, have also been reported to pose compatibilizing effect on immiscible polymers.[4,5] The reason is believed to be due to the hydrodynamic stabilization of the blend morphology by positioning of the nanoscale particles at the interface and suppressing minor phase droplets coalescence through reducing the interfacial tension.

The prominence of polypropylene (PP) as a commercial polymer enormously used in a great number of applications is beyond doubt. Nevertheless, it suffers from fundamental drawbacks in terms of thermal and mechanical properties aspects, which may narrow its scope of use. A practical resolution turned out to be blending PP with aromatic polyesters followed by compatibilization due to inherent immiscibility, whereby enhanced thermal, mechanical, and chemical resistance compared to plain PP are granted.[6–9] Because of an excellent combination of their favorable properties, poly(ethylene terephthalate) (PET), poly(butylene terephthalate), and in particular poly(trimethylene terephthalate) (PTT) are considered as the candidates of choice.[10] A greater improvement in the blend final

performance is still achieved when a nanolayered component is added into the system to deliver a blend nanocomposite.[11,12]

A consensus of relevant research states that morphological and rheological characteristics of multiphase polymer systems are mutually connected impressing the final material performance.[13] Hence, the morphological evolution and rheological properties of PP/aromatic polyesters blend nanocomposites have received some accounts. Calcagno et al.[14,15] observed that the clay nanoparticles show a better dispersion in PP/PET blends in the presence of a maleic compatibilizer, and finer droplets of PET are resulted upon the compatibilizer incorporation. Also, the nanoparticles were found to be selectively situated at the interphase and inside the polyester bulk. Upadhyay et al.[16] studied PTT/PP blend nanocomposites and reported that the addition of compatibilizer led to a more efficient dispersion of nanoscale reinforcements within the matrix. Elsewhere, Xue et al.[17] focused on the same system and reported that the domain size of the dispersed phase is decreased significantly with increasing the clay content. Also, the clay was found to be mainly distributed at the interface and show higher affinity toward PTT. In presence of the compatibilizer, much finer phase morphology was obtained.

In our recently published work,[18] the thermal and dynamic mechanical aspects of the PP/PTT blend nanocomposites were dealt with. The current effort is inspired as a continuation of our previously published paper which aims to qualitatively correlate the morphological characteristics of the melt-blended PP/PTT clay nanocomposites with the respective melt rheological properties. The influence of two different organoclay additives along with a functional compatibilizer in varying contents is also explored using electron microscopy, X-ray scattering technique, wettability analysis, and rheometry.

EXPERIMENTAL

Materials

Isotactic PP, grade Moplen HP501H with melt flow index of 2.1 g/10 min, was supplied by Basell Company (Germany). PTT, grade RTP 4700 with intrinsic viscosity of 0.901 mL/g, was purchased from RTP Company (USA). The zero-shear-rate viscosity values were found to be 2600 Pa s for PP and 1900 Pa s for PTT at 230°C. The compatibilizer was *n*-butyl acrylate glycidyl methacrylate ethylene terpolymer (commercially knows as Elvaloy PTW) containing 2.4 wt % glycidyl methacrylate (GMA) and obtained from DuPont with melt flow index of 12 g/10 min. Two types of organically modified montmorillonite (MMT), *viz.* Cloisite 30B and Cloisite 20A, were provided with Southern Clay Products.

Methods

The samples were prepared at 230°C inside a corotating, intermeshing, twin-screw extruder (diameter = 25 mm, length to diameter ratio = 36, Berstorff GmbH, Germany) at a screw speed of 200 rpm. A constant PP/PTT weight ratio of 75/25 was held with various amounts of the compatibilizer and organoclay as given in Table I.

Scanning electron microscopy (SEM) was performed on VEGA/TESCAN model operating at an accelerating voltage of 20 KV and magnification of 2000×. The specimens were cryogenically fractured in liquid nitrogen and sputter coated by a thin layer of gold-palladium alloy to enhance resolution. The micrographs were subsequently analyzed by image processing software to estimate number average radius (R_n), volume average radius (R_v), and particle size distribution (R_v/R_n) quantities based on around 400 droplets enumerated. Transmission electron microscopy (TEM) was also fulfilled on LEO 910 TEM (Carl Zeiss) at an accelerating voltage of 120 kV. Ultramicrotomy down to 80 nm thickness under cryogenic conditions at −120°C was carried out via EM UC/FC6 (Leica) equipped with a diamond knife.

Table I. Compositions and Symbols of the Samples Used Throughout the Work

Sample code	PP/PTT/Cloisite 30B/Cloisite 20A/Compatibilizer
B100	75/25/0/0
B95CB5	75/25/5/0/0
B95CA2.5CB2.5	75/25/2.5/2.5/0
B90E5CB5	75/25/5/0/5
B85E10CB5	75/25/5/0/10

Small angle X-ray scattering (SAXS) patterns were recorded on a S3-Micro Hecus diffractometer. The beam used Cu Ka radiation ($\lambda = 0.154$ nm), operated at 50 kVand 1 mA. The scanning was carried out in 2θ range from 0 to 10°.

Wettability analysis was carried out using contact angle measurements on Kruss G10 goniometer at 25°C with distilled water and diiodomethane as probe liquids, and the surface free energy values were evaluated using the instrument software based on the Owens/Wendt model.[19]

Rheological measurements were performed on a parallel plate MCR300 (Paar physica) at 240°C in oscillation mode under nitrogen ambient to prevent oxidative degradation. Linear viscoelastic region was found using strain sweep test. Frequency sweep experiments were then carried out over 0.01–600 rad/s at a strain of 30%, and rheological characteristics were then recorded.

RESULTS AND DISCUSSION

Morphology

In Figure 1, the SEM micrographs taken from different samples are presented. A droplet-like morphology is evident for the neat blend (B100), where in the PTT phase is finely dispersed. As the organoclay constituents are added into the blend (B95CB5 and B95CA2.5CB2.5 samples), the characteristic dispersed phase domain size decreases. This is also quantitatively shown in Table II, where a descending trend in number and volume average radii trend is visible. Cloisite 30B is apparently more capable than Cloisite 20A of making the phase morphology finer which can principally be related with its hydroxyethyl-containing structure. The compatibilizing mechanism of nanoclay is thought to be due to the presence of nanolayered moieties at the interface which hinder merging of the dispersed phase particles. However, the particle size distribution (R_v/R_n) is raised on the addition of both organoclay constituents which

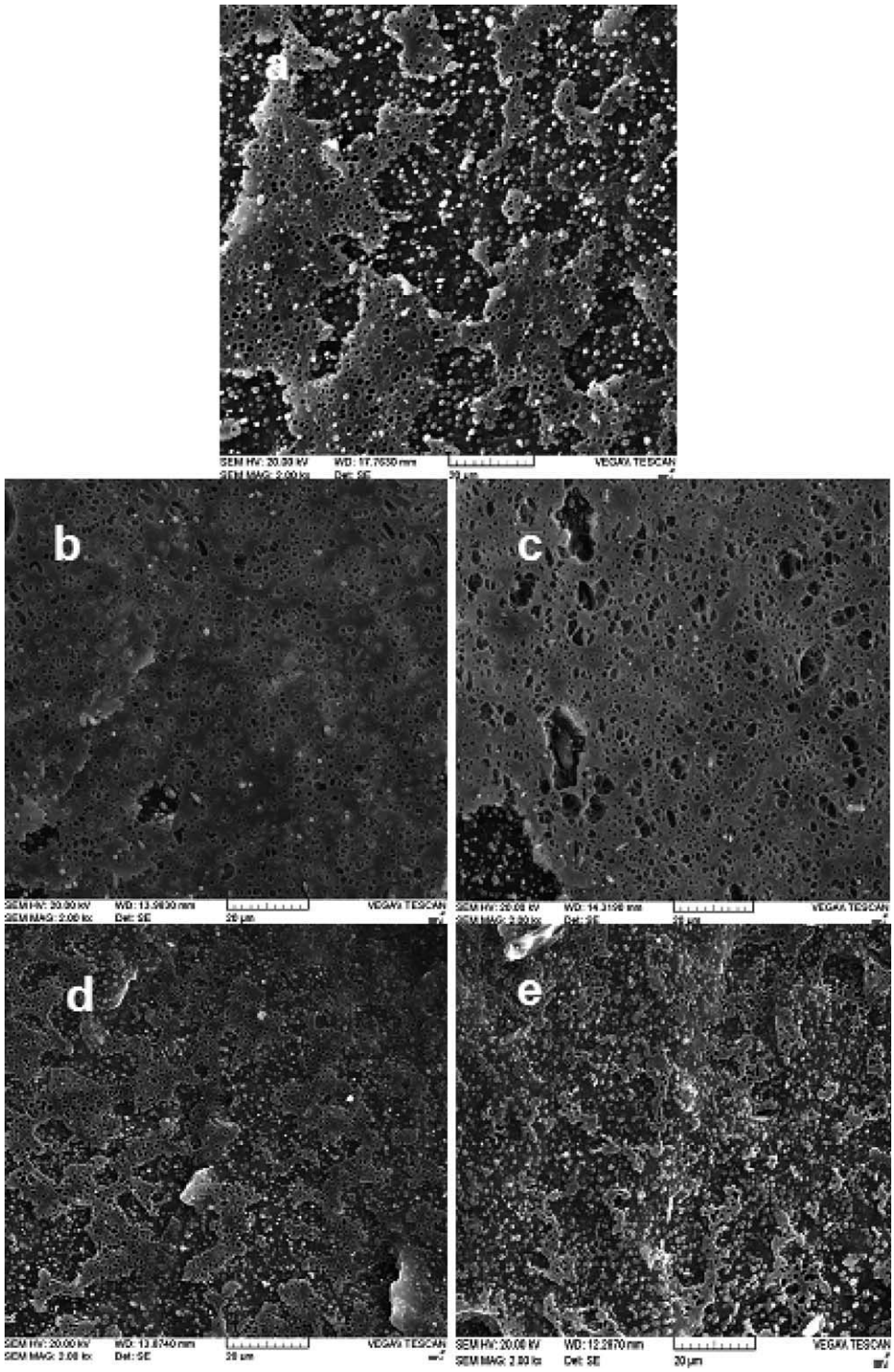

Figure 1. SEM images of various samples taken at 2000×, (a) B100, (b) B95CB5, (c) B95CA2.5CB2.5, (d) B90E5CB5, and (e) B85E10CB5.

could be explained such that the presence of nanoparticles causes to render a coarse interface and an irregular distribution of the dispersed phase, as reflected by increased R_v/R_n ratio. Further enhanced dispersion combined with better distribution is attained when the compatibilizer is incorporated into the system (B90E5CB5 and N85E10CB5 samples). Indeed, a more uniform surface morphology characteristic to a compatible blend is brought up. As expected, Elvaloy PTW is favorable for promotion of the interfacial adhesion between PP and PTT components. In fact, the interaction between functional groups of PTT and those of the compatibilizer gives a graft copolymer at the interface which improves the compatibility through interfacial tension reduction.[20]

Table II. Particle Size Characteristics of the Dispersed Phase (PTT)

Sample	R_n (μm)	R_v (μm)	R_v/R_n
B100	0.73	0.83	1.14
B95CB5	0.53	0.72	1.36
B95CA2.5CB2.5	0.58	1.10	2.00
B90E5CB5	0.47	0.55	1.18
B85E10CB5	0.45	0.50	1.10

Because of some instrumental limitations, SEM is unable to provide insight into the location of nanoclay particles in the system. To this end, an analysis of the surface free energy values together with TEM is required. In equilibrium state, the location of nanoparticles is governed by thermodynamics.[21] Generally, two situations are possible: (1) nanoparticles would be dispersed within the phase in which they have the most compatibility with and (2) nanoparticles would be localized at the interface of two phases provided the difference between thermodynamic properties of two polymers is small. To determine which situation governs, one can estimate the wetting parameter (W_a) defined as the difference of the surface tension between nanoclay and each polymeric constituent divided by the interfacial tension between two polymeric components. Surface tension may itself be calculated according to the proposed models available in the literature.[19] There are two extreme points for wetting parameter, namely +1 and −1, each corresponds to the localization of nanoscale aggregates inside one phase domain. In case the value falls between, a preferential positioning at the interfacial region is expected. The results from the above analysis are given in Table III. It is expected from the given data that Cloisite 20A should prefer to reside at the interface, whereas Cloisite 30B should select PTT phase under thermodynamic equilibrium circumstances.

TEM images from three nanoclay containing samples are indicated in Figure 2. A predominant, intercalated morphology from delaminated tactoids is mainly visible. Tactoids are defined as the bundle-like structures formed by many nanoparticles together whose the morphology differs from intercalated and exfoliated. It is observed from B95CB5 that Cloisite 30B prefers to be distributed within PTT phase due to the higher affinity. In contrast, Cloisite 20A is mainly located at the interface as expected from wettability data. The presence of Cloisite 20A particles at the interface leads to a decrease in coalescence. Introduction of the compatibilizer into the blend nanocomposite samples further modifies the prevailing morphology. The compatibilizer is observed form independent micelles, wherein Cloisite 30B is located which in turn diminishes the nanoclay content at the interface and inside the PTT droplets. Moreover, the compatibilizer decreases the droplets size while increasing their quantity because of the change it can induce in the interfacial tension and coalescence extent.

The SAXS patterns of different nanoclay-containing samples are illustrated in Figure 3. According to the literature,[22] the interlayer distances based on the Bragg's equation are 2.45 and 1.85 nm for Cloisite 20A and Cloisite 30B, respectively, which correspond to (001) plane. A visible shift of the characteristic signal toward low angles signifies enhanced gallery spacing related with the placement of the polymer chains between the nanoclay layers. Cloisite 30B functionalities maintain polar interactions with carboxyl and hydroxyl groups of PTT chains leading to a facilitated penetration of polymer chains through the clay galleries. Further interlayer distance together with more uniformly distributed particles is evident for compatibilizer-containing sample. The latter finding is concluded from a less broad characteristic peak for the sample which contains Elvaloy PTW. This behavior is indeed expected from the already given discussions on indisputable role of the compatibilizer.

Melt Rheology

The complex viscosity (η^*) as a function of the angular frequency (ω) for different samples are displayed in Figure 4. A shear-thinning behavior is demonstrated by each sample. The addition of the nanoclay yields a significant enhancement to the system viscosity which indeed stems from an additional friction as well as chain slippage restriction produced because of the organoclay particles located at the interface and inside dispersed phase.[23] The occurrence of physicochemical interactions between the polymeric constituent and the nanoclay also plays a critical role. This is reflected by the higher viscosity values of B95CB5 compared to B95CB2.5CA2.5, where in the former case stronger interactions between Cloisite 30B and PTT cause an extra restriction on the chain mobility. Further increase in viscosity is evident when the compatibilizer is also incorporated into the system which affects the phase morphology, as discussed earlier, thereby making the flow behavior change markedly. The underlying reason may be the finer dispersion, narrower particle size distribution, and enhanced interfacial adhesion induced by the compatibilizer.[24] The effect becomes even more pronounced as the Elvaloy PTW content is doubled. It is interesting to note that a Newtonian plateau comes out in the case of the neat blend at low frequencies which is almost vanished in presence of the additive-containing samples. In fact, the latter ones are involved in some interfacial interactions which consequently impress the rheological properties at very low frequencies. There arises an upturn in the curve which is supposed to originate from secondary structures formation as the very low-frequency range is highly sensitive to any interfacial phenomenon.[13]

Storage shear modulus (G') as a function of frequency sheds some light on the blends melt elasticity which is graphically

Table III. Data from Wettability Analysis of Neat Constituents and Nanoclays Based on the Contact Angle Measurement and Owens/Wendt Model[19]

Component	Γ^a (mN/m)	γ^{db} (mN/m)	Γ^{pc} (mN/m)	$d\gamma/dT^d$ (mN/m°C)	$W_a{}^e$
PP	30.1	30.1	0.0	−0.058	-
PTT	44.6	35.6	9.0	−0.065	-
Cloisite 30B	48.3	34.6	14.7	−0.1	−1.3
Cloisite 20A	42.1	31.8	10.3	−0.1	−0.9

[a]Surface free energy, [b]Dispersed part, [c]Polar part, [d]Temperature gradient of surface energy, [e]Evaluated at 230°C.

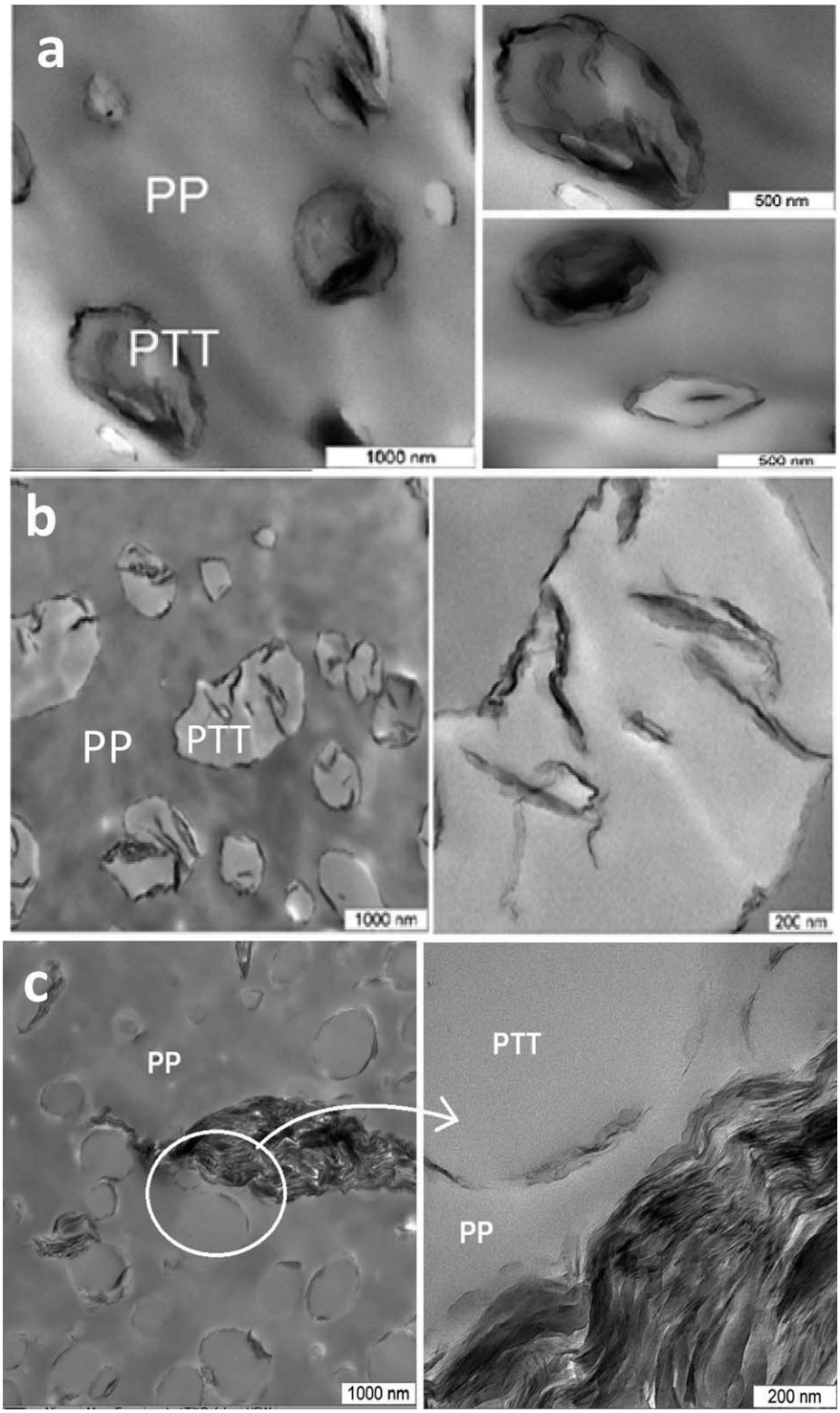

Figure 2. TEM images from different nanoclay-containing samples at various magnifications, (a) B95CB5, (b) B95CB2.5CA2.5, and (c) B90E10CB5.

represented in Figure 5. A typical ascending trend is detected in the case of the samples where the nanoclay is found to favor the system elasticity again ascribed to the morphological modifications and also polymer-nanoparticles interactions which bring forth the nanoscale reinforcement. This is more conspicuous for B95CB5 than B95CB2.5CB2.5 due to the stronger PTT–nanoclay interactions. Further increase in storage modulus is obvious subsequent to the compatibilizer addition which

Applied Polymer SCIENCE

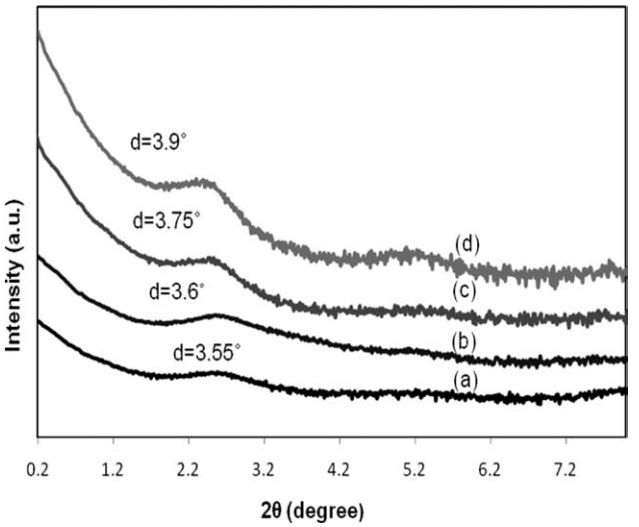

Figure 3. SAXS patterns of the samples, (a) B95CB5, (b) B95CA2.5CB2.5, (c) B90E5CB5, and (d) B85E10CB5.

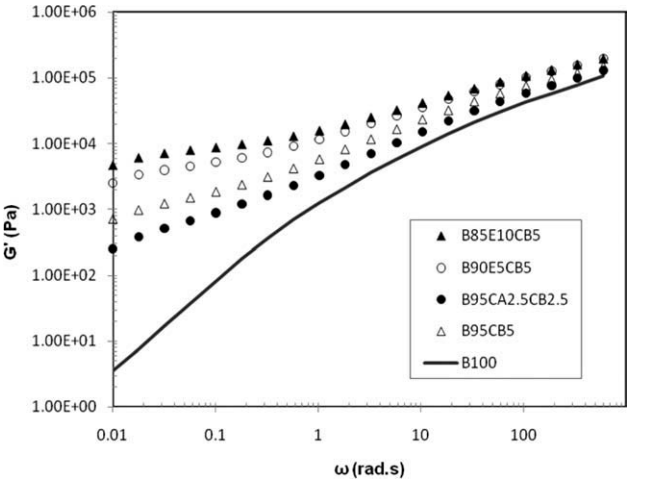

Figure 5. Storage shear modulus as a function of angular frequency for different samples.

influences the phase morphology, and in that connection, makes the melt elasticity change noticeably. This is accounted for by the finer dispersion, narrower particle size distribution, and improved interfacial binding evoked by the compatibilizer. It is worth noting that except for the neat blend, all the other samples exhibit a terminal plateau at very low angular frequency region which is believed to be a result of an intermolecular network in the system which has its own yield stress.[23,24] At higher frequencies, where the allocated time for the relaxation process is tighter, they are destroyed due to weak stability.

To gain an insight into the interfacial impact, it would be stimulating to have a look at the relaxation time distributions ($H(\lambda)$) obtained via storage shear moduli. Typically, a blend sample with an interphase gives an additional relaxation peak at extended times (very low frequency) due to the interface.[25] Based on Figure 6 which displays the relaxation time spectra ($\lambda H(\lambda)$ vs. λ), the pure blend shows just a single broad peak while the other samples which contain the nanoclay and compatibilizer possess additional peak at very high relaxation times associated with structured interface formed at very low frequency. The continuous relaxation time has been obtained according to the developed procedure already available in the literature.[26] This is further intensified for the compatibilizer-containing samples indicating the enlarged interfacial area due to the finer dispersed phase size and strengthened adhesion.

CONCLUSIONS

In this work, morphological and rheological properties of the melt-prepared PP/PTT at different concentrations of the compatibilizer and organically modified nanocomposites are dealt with. Contact angle analysis based on the wetting parameter approach is able to well predicate the location of the nanoclay particles within the system, confirmed by TEM. It is observed that the organoclay phase is preferentially distributed either at the interface or inside the PTT phase depending on the level of affinity. The organoclay phase also plays a compatibilizing role.

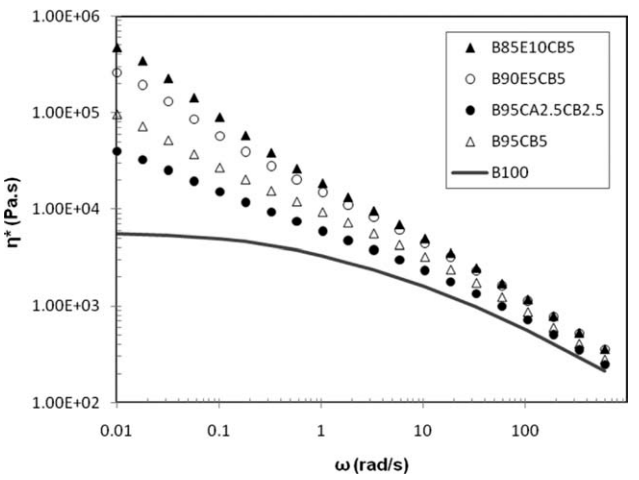

Figure 4. Complex viscosity curves as a function of angular frequency for different samples.

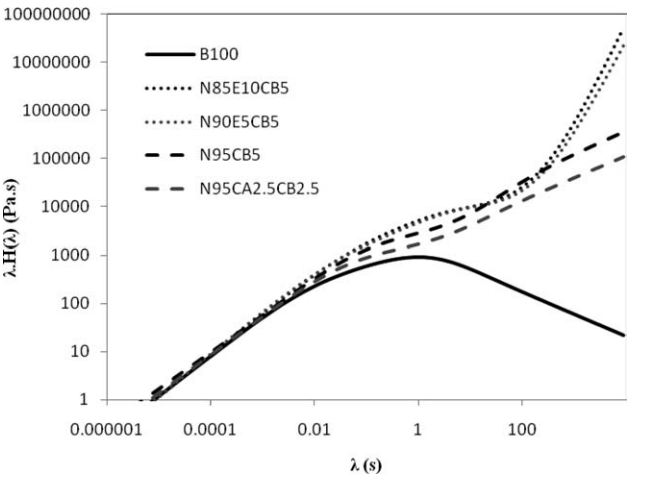

Figure 6. Relaxation time spectra for various samples evaluated based on G' plots.

SEM reveals that the functional compatibilizer gives rise to an enhanced interfacial adhesion and uniform morphology. Rheological measurements show that nanoclay and compatibilizer contribute to the complex viscosity of the system through chain mobility confinement. Also, an upturn is detected at low angular frequencies of the viscosity plots ascribed to the secondary structures formation. Similar behavior was also found when the storage shear modulus is taken into account, where at low frequencies a terminal plateau of yield stress character arises that is connected with some intermolecular networks formation. This can further be substantiated through relaxation time spectra, where additional peaks owing to structured interface emerge at high relaxation times.

ACKNOWLEDGMENTS

H. A. Khonakdar thanks Alexander von Humboldt foundation for financial support.

REFERENCES

1. Robeson, L. M. Polymer Blends: A Comprehensive Review; Hanser Verlag: Munich, **2007.**
2. Yavari, A.; Asadinezhad, A.; Jafari, S. H.; Khonakdar, H. A.; Ahmadian, S.; Böhme, F. *Macromol. Mater. Eng.* **2005,** *29*, 1091.
3. Jeon, H. S.; Nakatani, A. I.; Han, C. C.; Colby, R. H. *Macromolecules* **2000,** *33*, 9732.
4. Gelfer, M. Y.; Song, H. H.; Liu, L.; Hsiao, B. S.; Chu, B.; Rafailovich, M. *J. Polym. Sci.* **2003,** *41*, 44.
5. Cho, S.; Hong, J. S.; Lee, S. J.; Ahn, K. H.; Covas, J. A.; Maia, J. K. *Macromol. Mater. Eng.* **2011,** *296*, 341.
6. Xanthos, M.; Young, M. W.; Biesenberger, J. A. *Polym. Eng. Sci.* **1990,** *30*, 55.
7. Jayanarayanan, K.; Bhagawan, S. S.; Thomas, S.; Joseph, K. *Polym. Bull.* **2008,** *60*, 525.
8. Kordjazi, Z.; Golshan Ebrahimi, N. *J. Appl. Polym. Sci.* **2010,** *116*, 441.
9. Koysuren1, O.; Yesil, S.; Bayram, G. *J. Appl. Polym. Sci.* **2010,** *118*, 3041.
10. Khonakdar, H. A.; Jafari, S. H.; Asadinezhad, A. *Iran. Polym. J.* **2008,** *17*, 19.
11. Boudenne, A. Handbook of Multiphase Polymer Systems; Wiley: New York, **2011.**
12. Mittal, V. Advances in Polyolefin Nanocomposites; CRC Press: New York, **2011.**
13. Utracki, L.A. Polymer Blends Handbook, Vol. 1; Springer Verlag: Munich, **2002.**
14. Calcagno, C. I. W.; Mariani, C. M.; Teixeira, S. R.; Mauler, R. S. *Compos. Sci. Technol.* **2008,** *68*, 2193.
15. Calcagno, C. I. W.; Mariani, C. M.; Teixeira, S. R.; Mauler, R. S. *J. Appl. Polym. Sci.* **2009,** *111*, 29.
16. Upadhyay, D.; Mohanty, S.; Nayak, S. K.; Parvaiz, M. R.; Panda, B. P. *J. Appl. Polym. Sci.* **2011,** *120*, 932.
17. Xue, M. L.; Li, P. *J. Appl. Polym. Sci.* **2009,** *113*, 3883.
18. Jafari, S. H.; Kalati-vahid, A.; Khonakdar, H. A.; Asadinezhad, A.; Wagenknecht, U.; Jehnichen, D. *Express Polym. Lett.* **2012,** *6*, 148.
19. Owens, D. K.; Wendt, R. C. *J. Appl. Polym. Sci.* **1969,** *13*, 1741.
20. Entezam, M.; Khonakdar, H. A.; Yousefi, A. A.; Jafari, S. H.; Wagenknecht, U.; Heinrich, G.; Kretzschmar, B. *Macromol. Mater. Eng.* **2012,** *297*, 312.
21. Huang, W. Y.; Liu, C.; Chen, X.; Yang, Q.; Li, G. *Colloid Polym. Sci.* **2010,** *288*, 753.
22. Smart, G.; Kandola, B. K.; Richard Horrocks, A.; Nazaré, S.; Marney, D. *Polym. Adv. Technol.* **2008,** *19*, 658.
23. Jafari, S. H.; Yavari, A.; Asadinezhad, A.; Khonakdar, H. A.; Boehme, F. *Polymer* **2005,** *46*, 5082.
24. Sengers, W. G. F.; Sengupta, P.; Noordermeer, J. W. M.; Picken, S. J.; Gotsis, A. D. *Polymer* **2004,** *45*, 8881.
25. Riemann, R. E.; Cantow, H. J.; Friedrich, C. *Macromolecules,* **1997,** *30*, 5476.
26. Ward, I. M.; Sweeney, J. An Introduction to the Mechanical Properties of Solid Polymers; Wiley: New York, **2004.**
27. Wang, Y.; Zhang, Q.; Fu, Q. *Macromol. Rapid Commun.* **2003,** *24*, 231.
28. Iza, M.; Bousmina, M.; Jérôme, R. *Rheol. Acta* **2001,** *40*, 10.